An Implicit Method for Extended MHD using Adaptive, High-Order, High-Continuity Finite Elements

S. C. Jardin, J. Breslau, N. Ferraro, and M3D team
Princeton Plasma Physics Laboratory

A. Bauer, M. Shephard
Rensselaer Polytechnic Institute

FDM3D Meeting

PPPL

March 19-21 2007

The Extended MHD equations for a magnetized (fusion) plasma are a high-order system of 8 scalar variables that are characterized by a wide range of space and timescales.

The M3D-C^1 approach is as follows:

Multiple space scales $\rightarrow$ unstructured adaptive elements

Multiple time scales $\rightarrow$ implicit time differencing

High order derivatives $\rightarrow$ C^1 continuity elements (up to 4th order)

8 scalar variables $\rightarrow$ split implicit time advance & compact rep.

Strong magnetic field $\rightarrow$ stream function/potential representation

Extended MHD Equations:

$$\frac{\partial n}{\partial t} + \nabla \bullet (n\vec{V}) = 0$$

$$\frac{\partial \vec{B}}{\partial t} = -\nabla \times \vec{E} \qquad \vec{J} = \nabla \times \vec{B}$$

$$\vec{V} = \nabla U \times \hat{z} + \nabla_\perp \chi + V_z$$

$$\vec{B} = \nabla \psi \times \hat{z} + I\hat{z}$$

$$nM_i\left(\frac{\partial \vec{V}}{\partial t} + \vec{V} \bullet \nabla \vec{V}\right) + \nabla p = \vec{J} \times \vec{B} - \nabla \bullet \Pi_{GV} + \mu \nabla^2 \vec{V}$$

$$\vec{E} + \vec{V} \times \vec{B} = \eta \vec{J} + \frac{1}{ne}\left(\vec{J} \times \vec{B} - \nabla p_e\right) - \lambda_H (\Delta x)^2 \nabla^2 \vec{J}$$

$$\frac{3}{2}\frac{\partial p_e}{\partial t} + \nabla \bullet \left(\frac{3}{2} p_e \vec{V}\right) = -p_e \nabla \bullet \vec{V} + \eta J^2 + \frac{\vec{J}}{ne} \bullet \left[\frac{3}{2}\nabla p_e - \frac{5}{2}\frac{p_e}{n}\nabla n\right] - \nabla \bullet \vec{q}_e + Q_\Delta$$

$$\frac{3}{2}\frac{\partial p_i}{\partial t} + \nabla \bullet \left(\frac{3}{2} p_i \vec{V}\right) = -p_i \nabla \bullet \vec{V} + \mu \left|\nabla V\right|^2 - \nabla \bullet \vec{q}_i - Q_\Delta$$

8 scalar variables: $\psi, I, U, \chi, V_z, n, p_e, p_i$

Δx is typical zone (element) size

Scalar data is represented using 18 degree of freedom quintic triangular finite elements Q_{18}

- All data is at nodes: function + first 5 derivatives (6 DOF)

- Complete quintic polynomial has 21 coefficients

  - 18 values come from the 3 nodes (3 x 6)

  - 3 values come from requirement that the normal derivative along each edge be only a (univariate) cubic….leads to C^1 continuity

- Contains a complete Taylor series through 4th order…error ~ h^5

- Compact representation … only 3 DOF/triangle

- C^1 continuity allows up to 4th derivatives in space without introducing auxiliary variables

- Unstructured triangular mesh allows adaptive zoning

Φ

Φ_x

Φ_y

Φ_{xx}

Φ_{xy}

Φ_{yy}
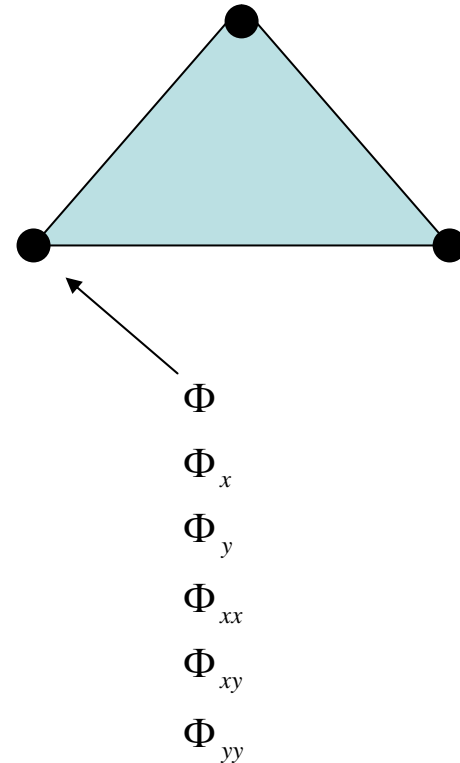
Implicit velocity time-advance substitutes in from field equations to contain all Ideal MHD wave phenomena

$$\rho\dot{\vec{V}} = \left(\vec{J} + \theta\delta t\dot{\vec{J}}\right)\times\left(\vec{B} + \theta\delta t\dot{\vec{B}}\right) - \nabla\left(P + \theta\delta t\dot{P}\right) + \cdots$$

$$\dot{\vec{J}} = \nabla\times\nabla\times\left[\left(\vec{V} + \theta\delta t\dot{\vec{V}}\right)\times B\right] + \cdots$$

$$\dot{\vec{B}} = \nabla\times\left[\left(\vec{V} + \theta\delta t\dot{\vec{V}}\right)\times B\right] + \cdots$$

$$\dot{P} = -\left(\vec{V} + \theta\delta t\dot{\vec{V}}\right)\bullet\nabla P - \frac{5}{3}P\nabla\bullet\left(\vec{V} + \theta\delta t\dot{\vec{V}}\right)$$

let $\dot{\vec{V}} = \dfrac{\vec{V}^{n+1} - \vec{V}^{n}}{\delta t}$, move all $\vec{V}^{n+1}$ terms to left side of equation

$$L_1\left\{V^{n+1}\right\} = L_2\left\{V^{n}\right\} + \cdots$$

Unconditionally Stable for $\theta \geq 0.5$

Use SuperLU_dist to invert this linear operator to get from time n to (n+1)

A similar technique is used on the magnetic field equations. Fully implicit Extended MHD (2-fluid) equations-- time step determined by accuracy only:

$$
\begin{bmatrix} S_{11}^{v} & S_{12}^{v} & S_{13}^{v} \\ S_{21}^{v} & S_{22}^{v} & S_{23}^{v} \\ S_{31}^{v} & S_{32}^{v} & S_{33}^{v} \end{bmatrix} \bullet \begin{bmatrix} U \\ V_z \\ \chi \end{bmatrix}^{n+1} = \begin{bmatrix} D_{11}^{v} & D_{12}^{v} & D_{13}^{v} \\ D_{21}^{v} & D_{22}^{v} & D_{23}^{v} \\ D_{31}^{v} & D_{32}^{v} & D_{33}^{v} \end{bmatrix} \bullet \begin{bmatrix} U \\ V_z \\ \chi \end{bmatrix}^{n} + \begin{bmatrix} R_{11}^{v} & R_{12}^{v} & R_{13}^{v} \\ R_{21}^{v} & R_{22}^{v} & R_{23}^{v} \\ R_{31}^{v} & R_{32}^{v} & R_{33}^{v} \end{bmatrix} \bullet \begin{bmatrix} \psi \\ I \\ P_e \end{bmatrix}^{n}
$$

$$
\vec{V} = \nabla U \times \hat{z} + \nabla_{\perp} \chi + V_z
$$
$$
\vec{B} = \nabla \psi \times \hat{z} + I \hat{z}
$$

Alfven Wave physics

$$
S_{11}^{n} \bullet N^{n+1} = D_{11}^{n} \bullet N^{n} + \begin{bmatrix} R_{11}^{n} & R_{12}^{n} & R_{13}^{n} \end{bmatrix} \bullet \begin{bmatrix} U \\ V_z \\ X \end{bmatrix}^{n+1} + \begin{bmatrix} Q_{11}^{n} & Q_{12}^{n} & Q_{13}^{n} \end{bmatrix} \bullet \begin{bmatrix} U \\ V_z \\ X \end{bmatrix}^{n} + Q_{14}^{n}
$$

density

$$
S_{11}^{p} \bullet P^{n+1} = D_{11}^{p} \bullet P^{n} + \begin{bmatrix} R_{11}^{p} & R_{12}^{p} & R_{13}^{p} \end{bmatrix} \bullet \begin{bmatrix} U \\ V_z \\ X \end{bmatrix}^{n+1} + \begin{bmatrix} Q_{11}^{p} & Q_{12}^{p} & Q_{13}^{p} \end{bmatrix} \bullet \begin{bmatrix} U \\ V_z \\ X \end{bmatrix}^{n} + Q_{14}^{p}
$$

pressure

$$
\begin{bmatrix} S_{11}^{p} & S_{12}^{p} & S_{13}^{p} \\ S_{21}^{p} & S_{22}^{p} & S_{23}^{p} \\ S_{31}^{p} & S_{32}^{p} & S_{33}^{p} \end{bmatrix} \bullet \begin{bmatrix} \psi \\ I \\ P_e \end{bmatrix}^{n+1} = \begin{bmatrix} D_{11}^{p} & D_{12}^{p} & D_{13}^{p} \\ D_{21}^{p} & D_{22}^{p} & D_{23}^{p} \\ D_{31}^{p} & D_{32}^{p} & D_{33}^{p} \end{bmatrix} \bullet \begin{bmatrix} \psi \\ I \\ P_e \end{bmatrix}^{n} + \begin{bmatrix} R_{11}^{p} & R_{12}^{p} & R_{13}^{p} \\ R_{21}^{p} & R_{22}^{p} & R_{23}^{p} \\ R_{31}^{p} & R_{32}^{p} & R_{33}^{p} \end{bmatrix} \bullet \begin{bmatrix} U \\ V_z \\ \chi \end{bmatrix}^{n+1} + \begin{bmatrix} Q_{11}^{p} & Q_{12}^{p} & Q_{13}^{p} \\ Q_{21}^{p} & Q_{22}^{p} & Q_{23}^{p} \\ Q_{31}^{p} & Q_{32}^{p} & Q_{33}^{p} \end{bmatrix} \bullet \begin{bmatrix} U \\ V_z \\ \chi \end{bmatrix}^{n}
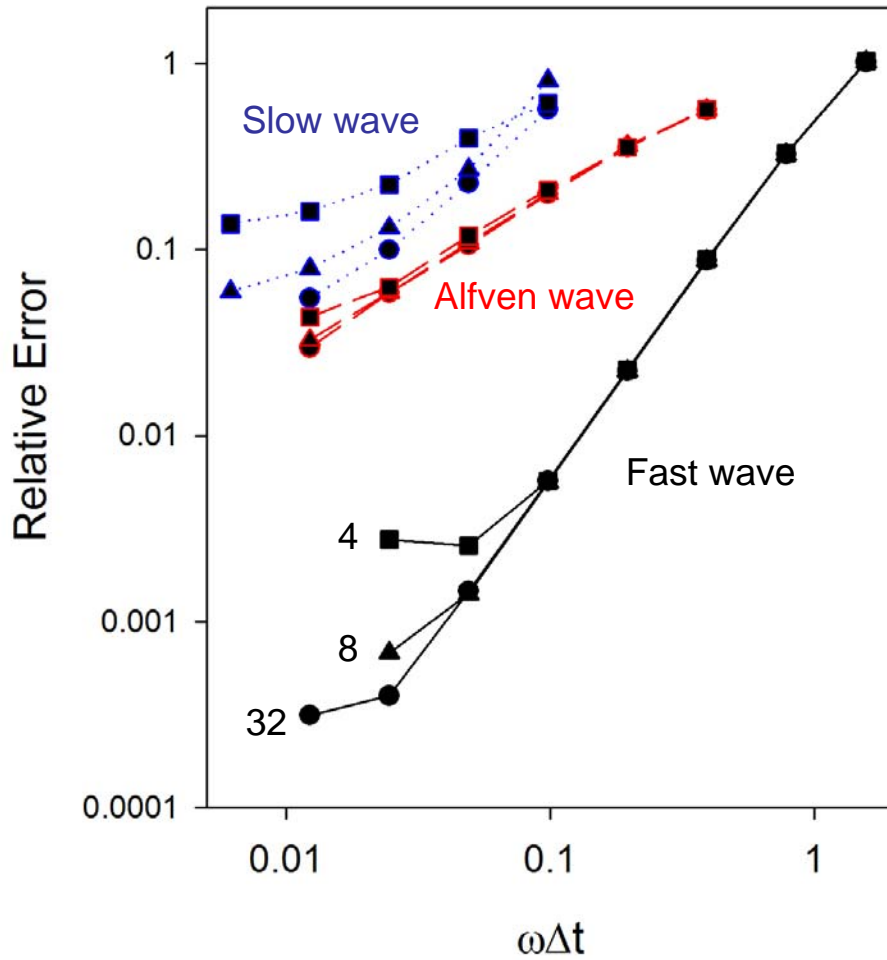$$

Whistler, KAW, field diffusion physics

- 4 sequential matrix solves per time step

- 3 non-trivial subsets with 6,4,2 variables

Start system in an eigenmode for a propagating Whistler wave, let it propagate 1 wavelength, and calculate RMS error between final and initial state. Doubly periodic
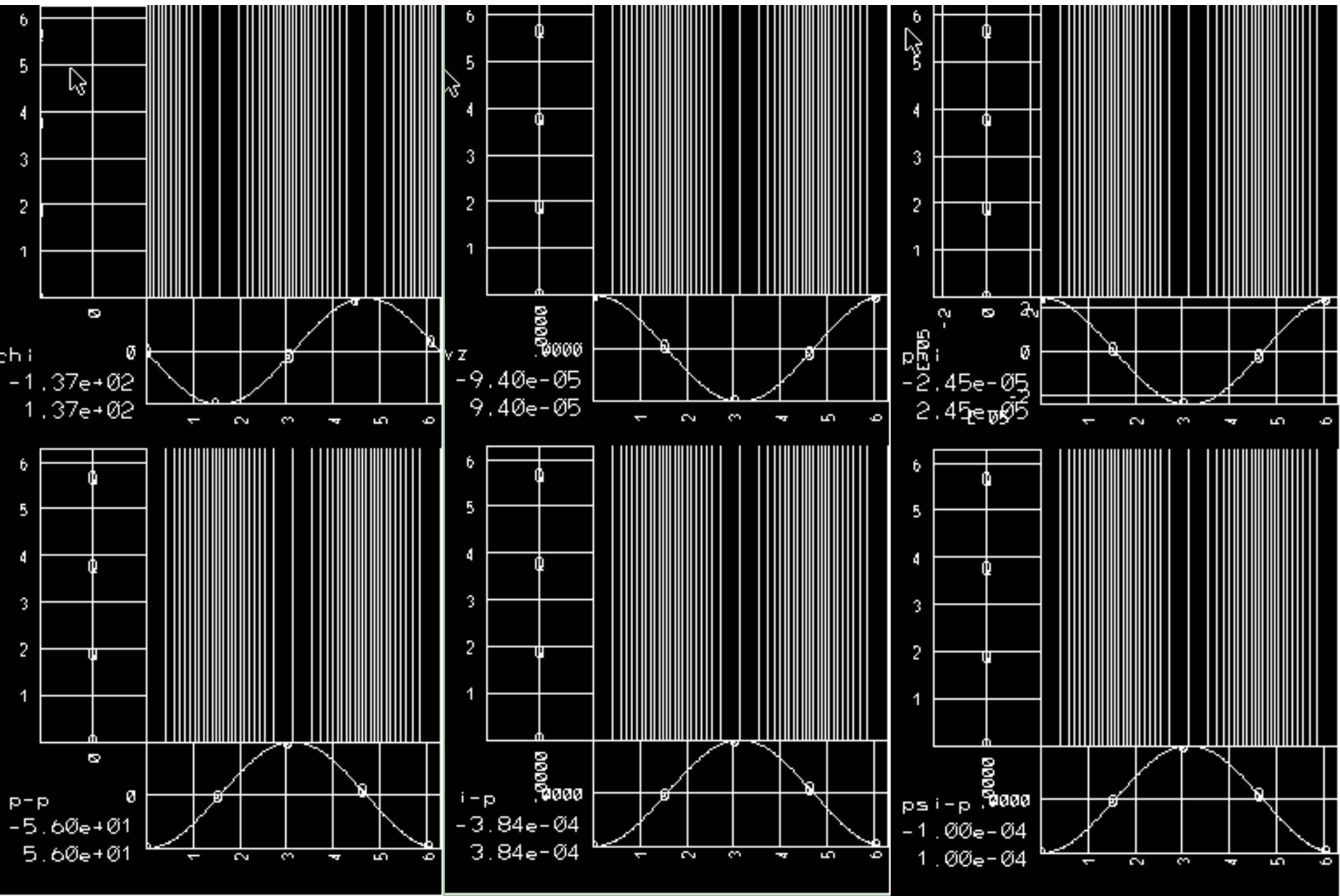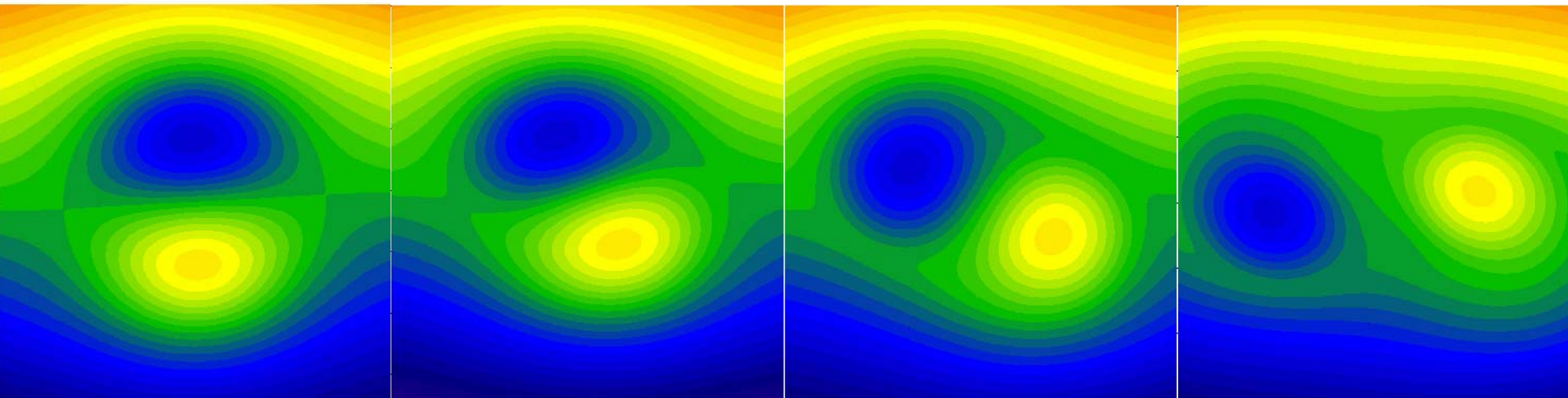
Plane Wave Convergence Test

θ is implicit parameter: $\theta=0.5$ is time centered

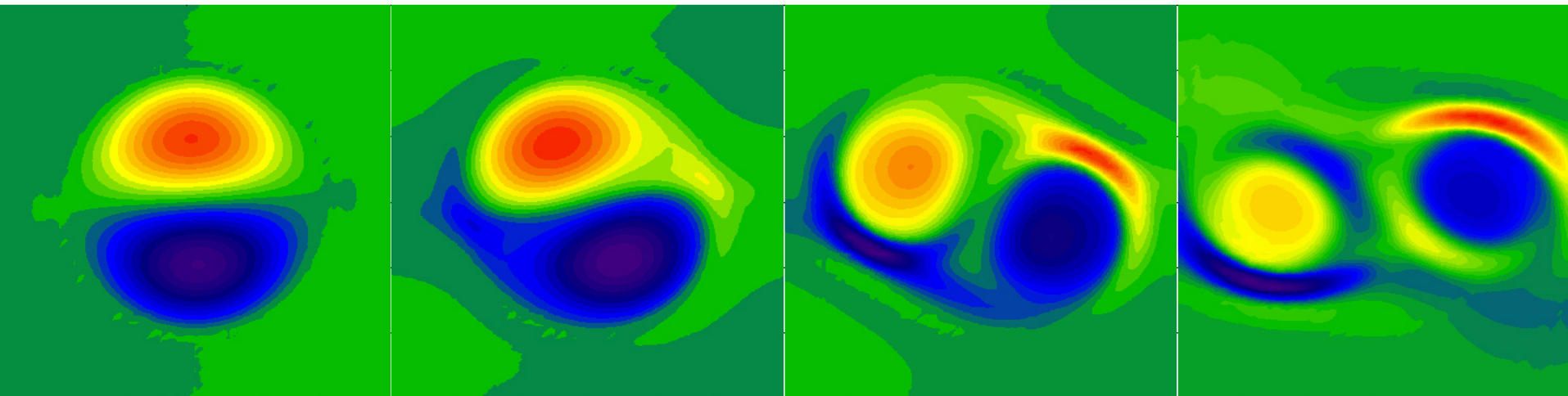# Non-linear evolution of tilting cylinder in full 6-field 2-fluid model

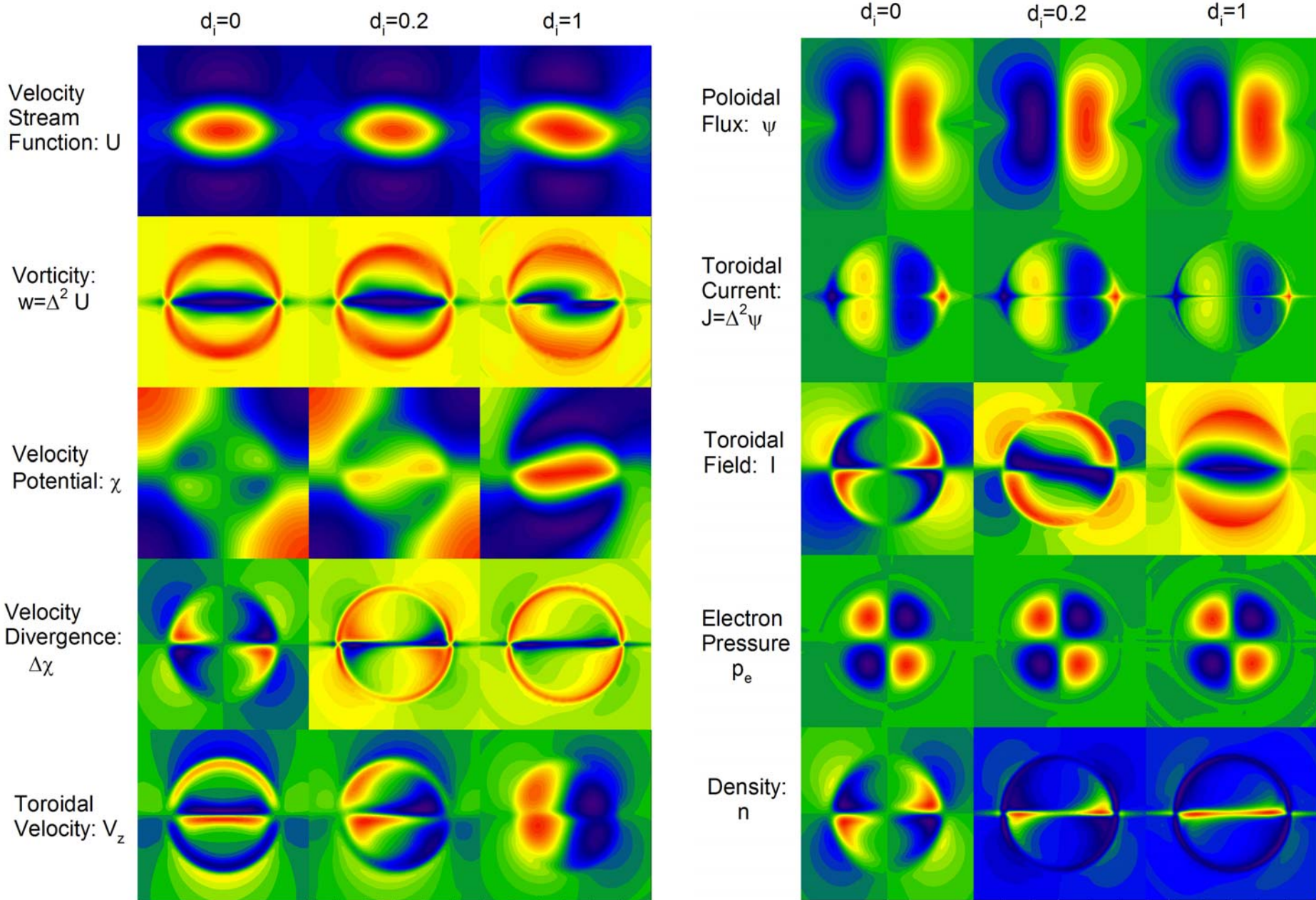Ψ: t=0.8 Ψ: t=3.8 Ψ: t=4.0 Ψ: t=4.8
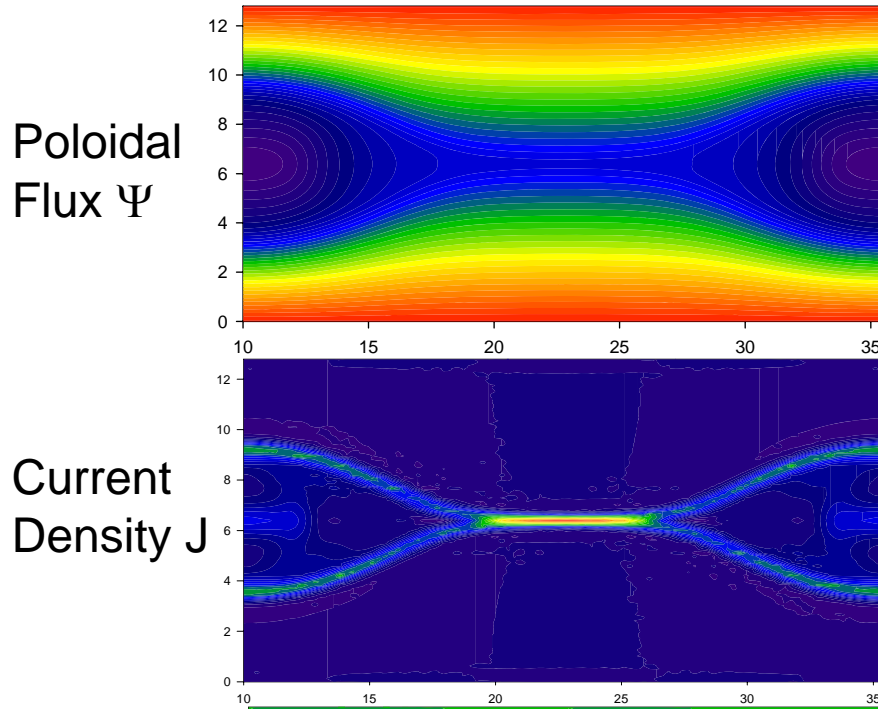
J: t=0.8   J: t=3.2   J: t=4.0   J: t=4.8

Tilting Cylinder Linear Eigenfunctions as a function of ion-skin depth parameter
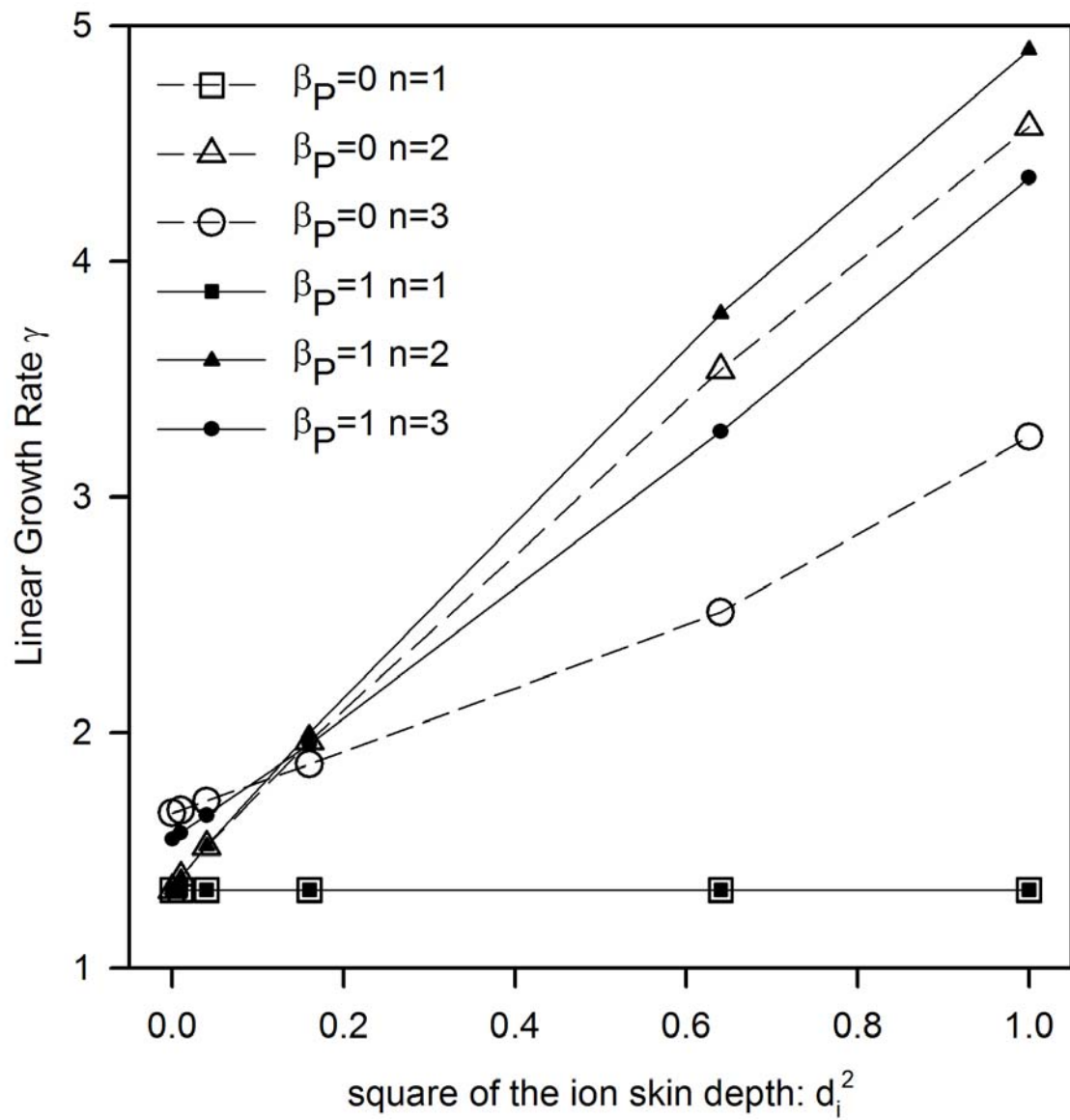
GEM Nonlinear Benchmark

Poloidal Flux Ψ

Current Density J

GEM Reconnection Problem

$$\psi^0(x, y) = \frac{1}{2}\ln(\cosh 2y)$$

$$P^0(x, y) = \left[\sec h^2 2y + 0.2\right]$$

$$\tilde{\psi}(x, y) = \varepsilon \cos k_x x \cos k_y y$$

1. Resistive MHD
   High and Low Viscosity
   ($\mu = 10\ \eta$, $\mu = 0.1\ \eta$)

2. Two-Fluid

• Provides a non-trivial, convenient test problem for code verification and validation and cross-code comparison

• Also, extending this by adding an equilibrium magnetic field into the plane (guide field)

J.Birn, J.F.Drake, M.A. Shay *et al.*,J. Geophys. Res. **106** 3715 (2001)

Current Density contours for 2-fluid MHD
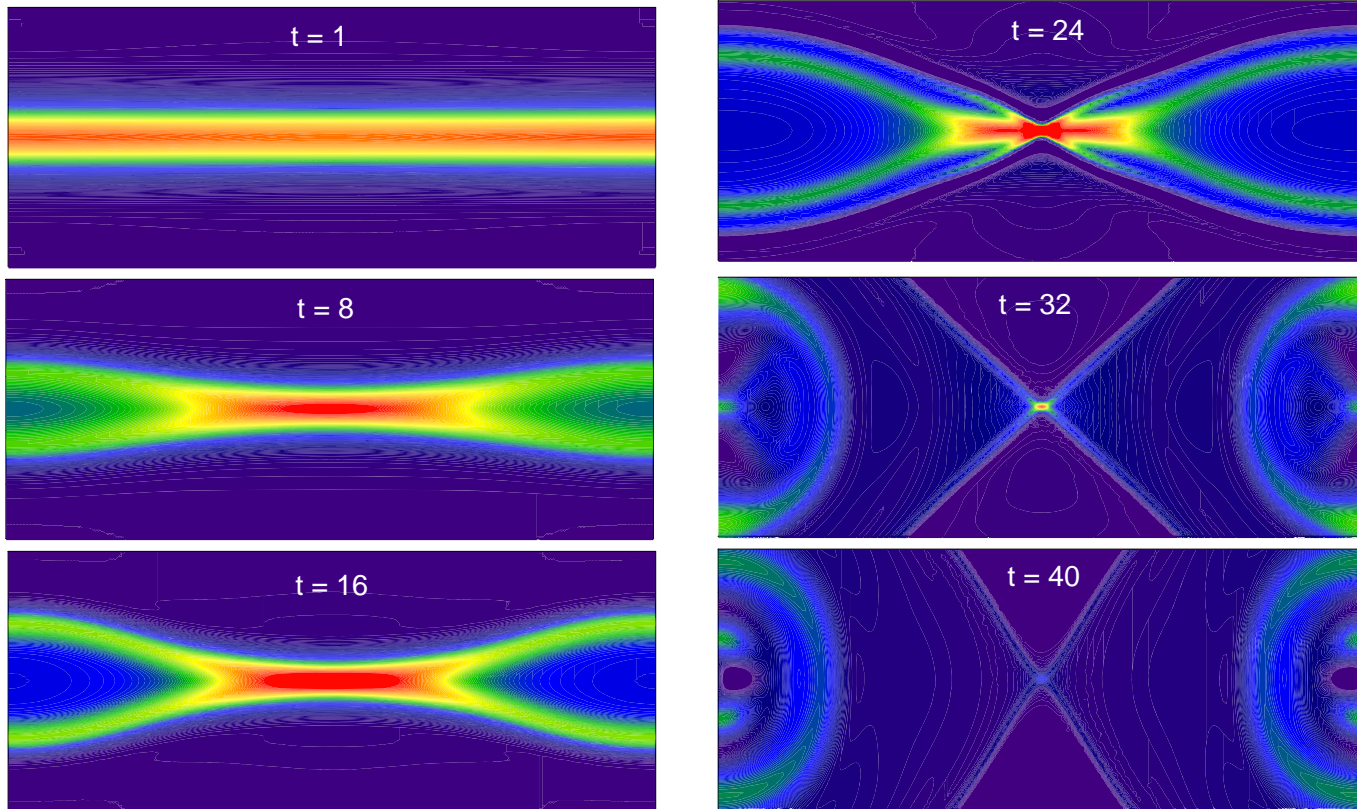
- Starts like resistive MHD

- Dramatic change in configuration for t > 20
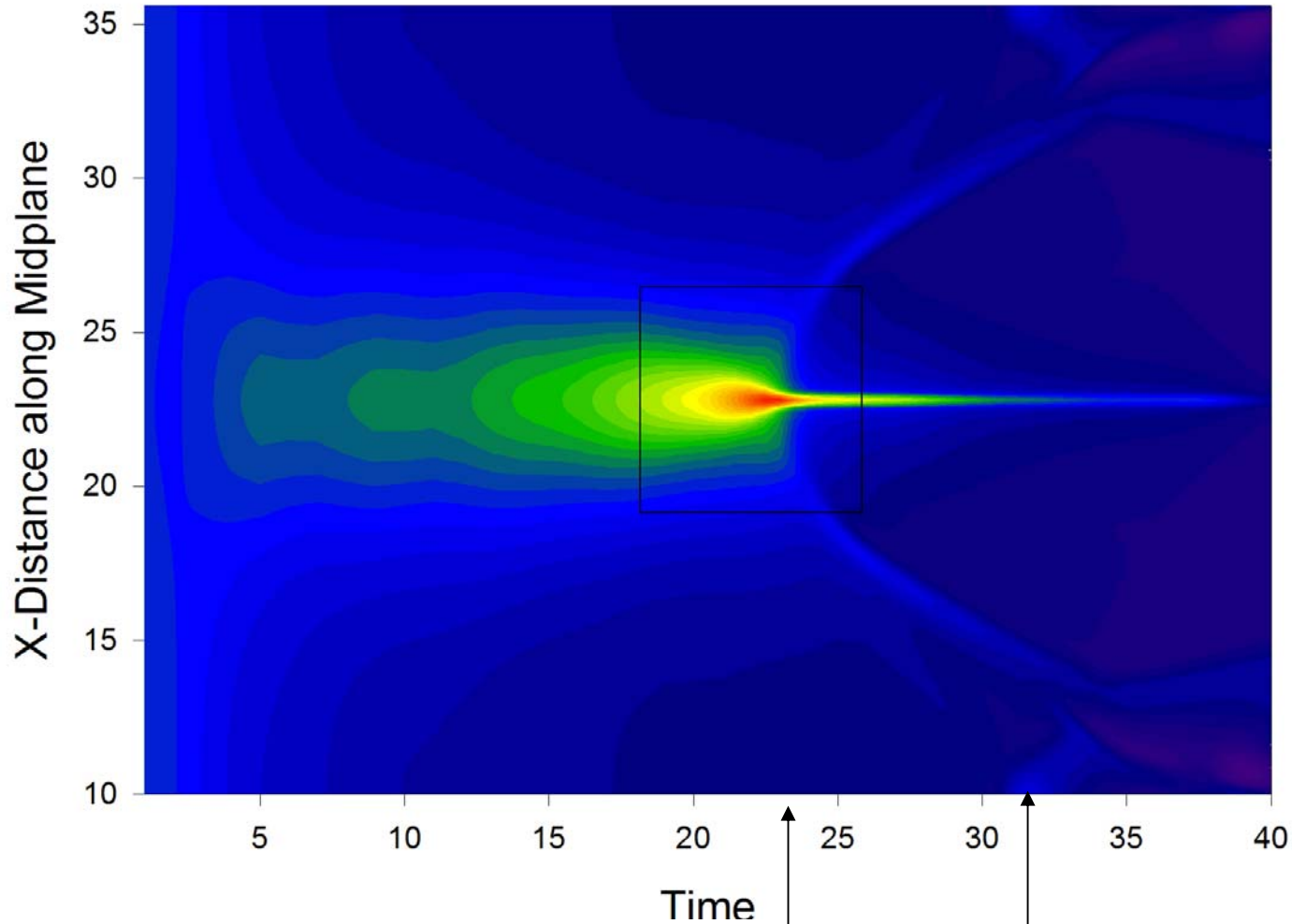
Close-up of 2-fluid current density at t=32

t=32
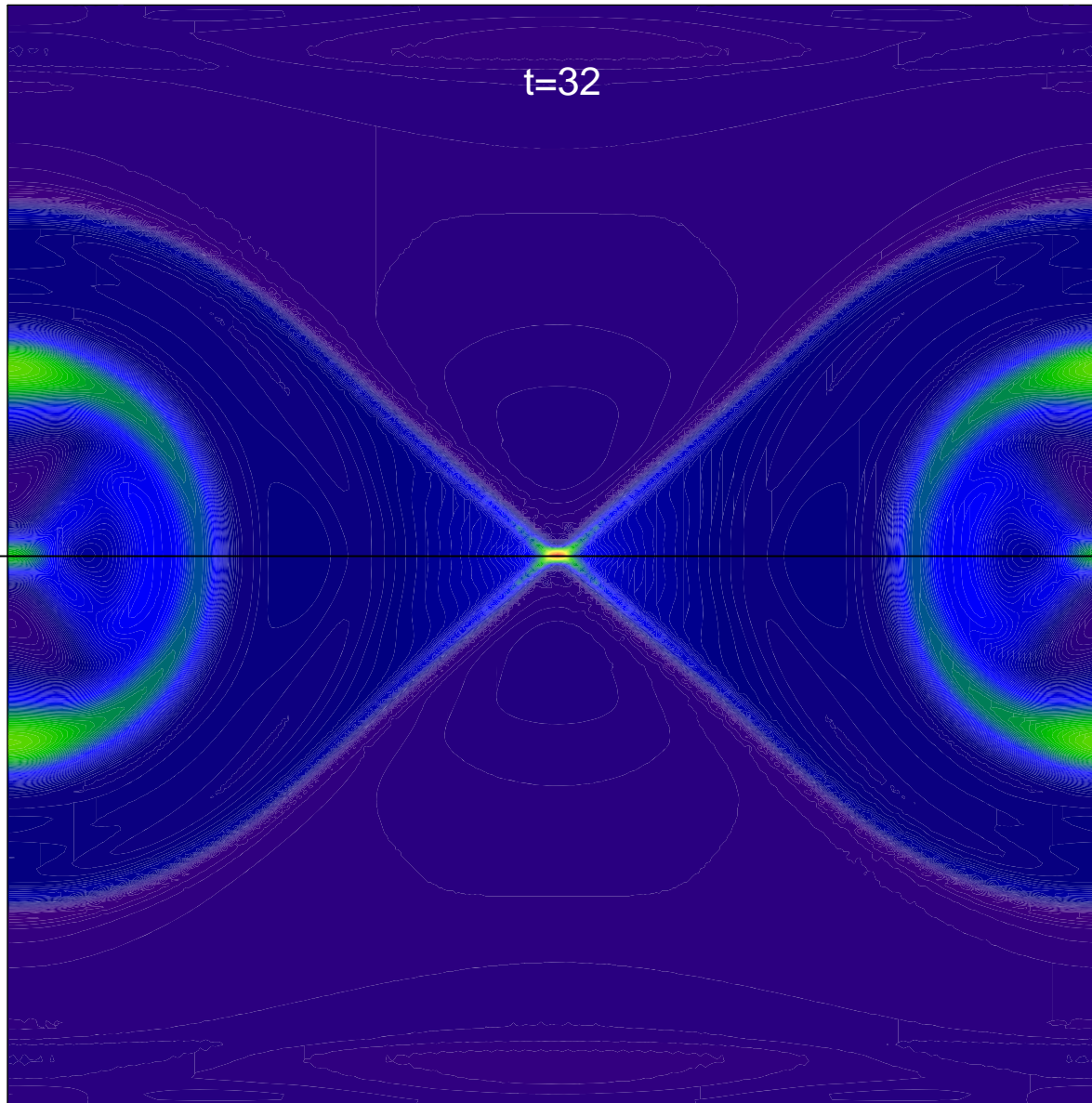
midplane

• Note very localized region of high current density in center

These calculations did not assume any symmetry, except for initial and boundary conditions

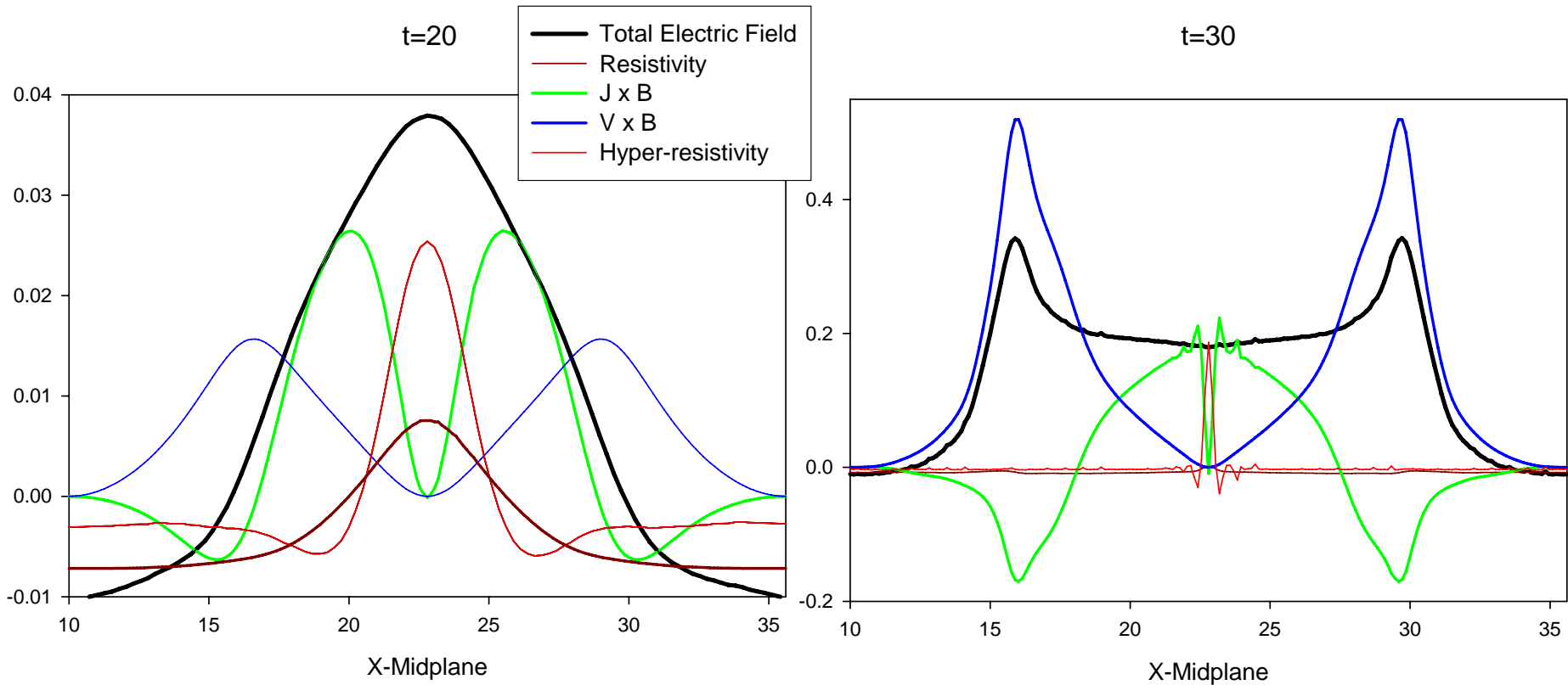# Midplane Current density collapses to the width of 1-3 triangular elements

t=32 time of previous contour plot
(note sudden collapse at t=23+)
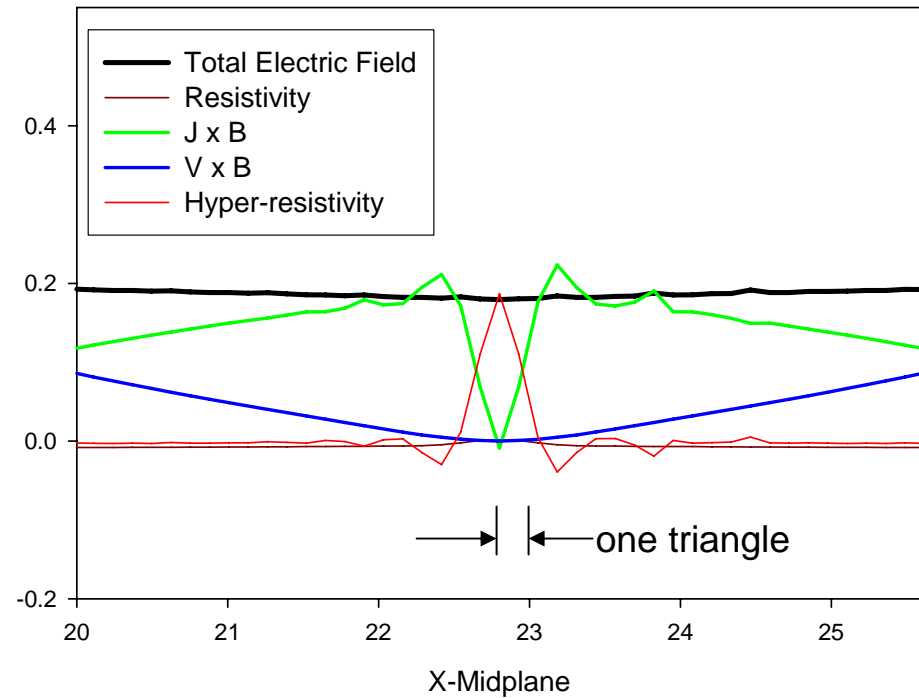
Blowup of Midplane Current density vs time
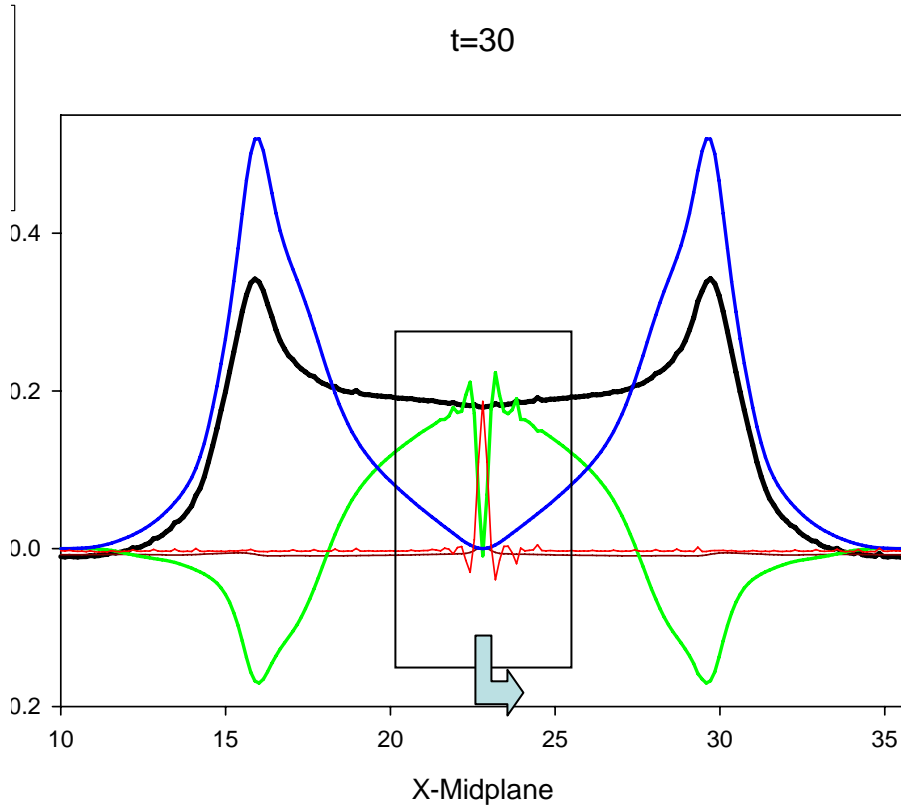

Time

X-Distance along Midplane

Time
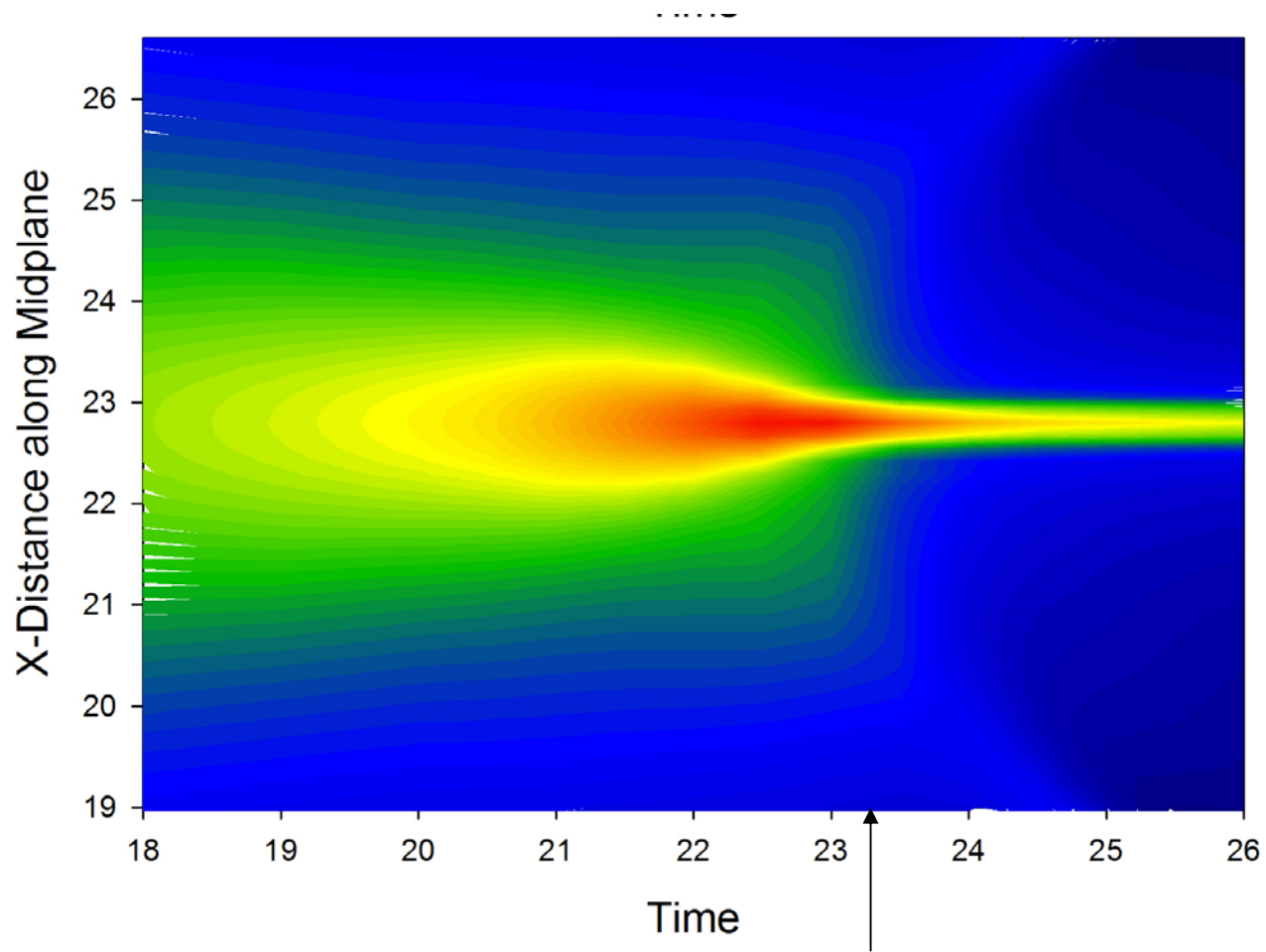
(note sudden collapse at t~23+)

Midplane electric field before and after transition

Reconnection rate: $\hat{z} \bullet \left[\vec{E} = -\vec{V} \times \vec{B} + \eta \vec{J} + \frac{1}{ne} \left(\vec{J} \times \vec{B} - \nabla p_e \right) - \lambda_H (\Delta x)^2 \nabla^2 \vec{J} \right]$

Blowup showing electric field after transition

t=30

Legend:
- **Total Electric Field** (black, bold)
- Resistivity (dark red)
- J x B (green)
- V x B (blue)
- Hyper-resistivity (red)

X-Midplane

one triangle

$$\hat{z} \bullet \left[\vec{E} = -\vec{V} \times \vec{B} + \eta \vec{J} + \frac{1}{ne}\left(\vec{J} \times \vec{B} - \nabla p_e \right) - \lambda_H (\Delta x)^2 \nabla^2 \vec{J} \right]$$

Hyper-resistivity coefficient must be large enough that current density collapse is limited to 1-2 triangles: *reason for factor (Δx)²*

2-fluid reconnection requires high resolution for convergent results

• Note sudden transition where velocity abruptly increases

•These calculations used a hyperviscosity term in Ohm's law proportional to $(\Delta x)^{2 \cdots}$ required for a stable calculation
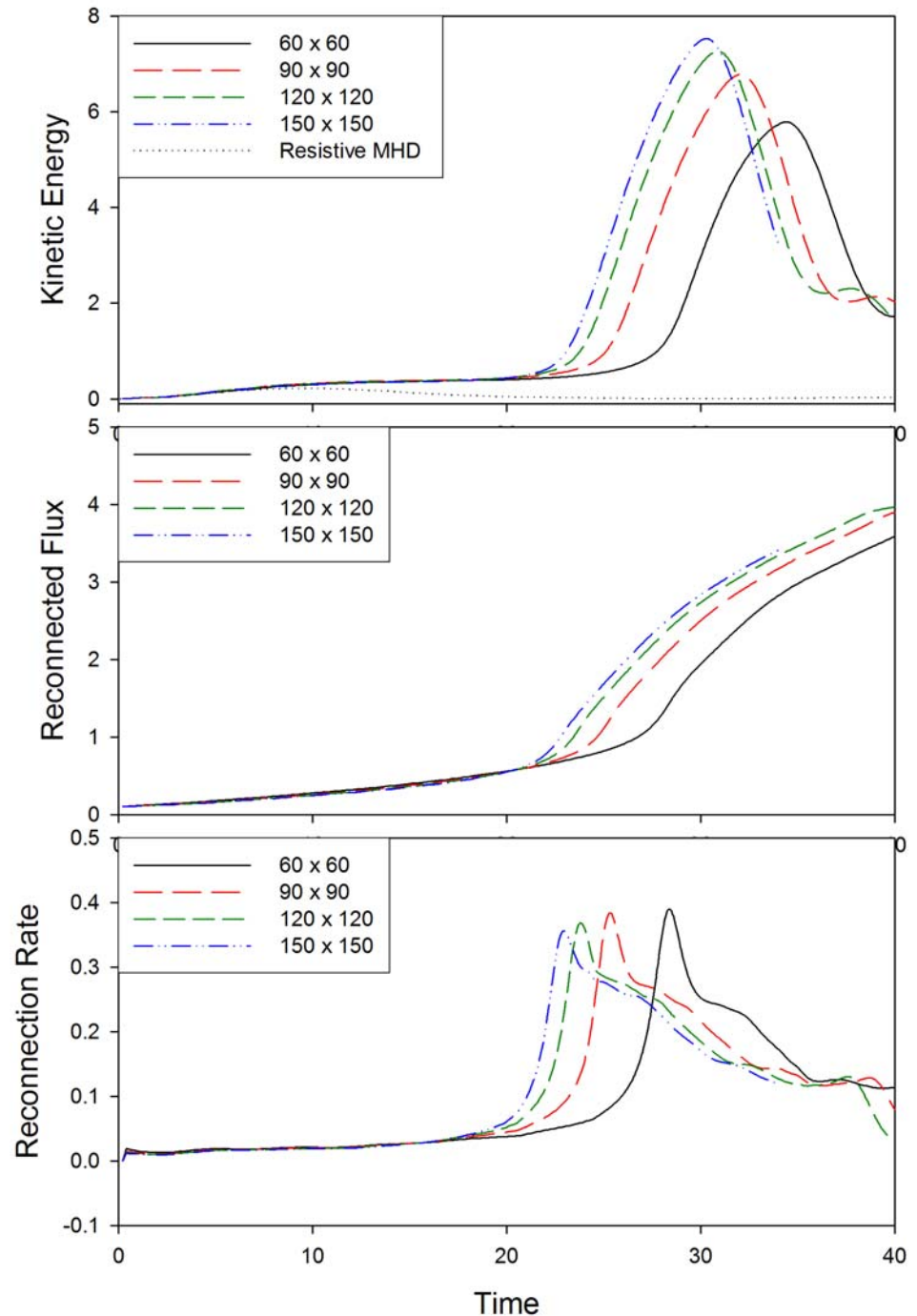
Results are converging

Convergence Graph
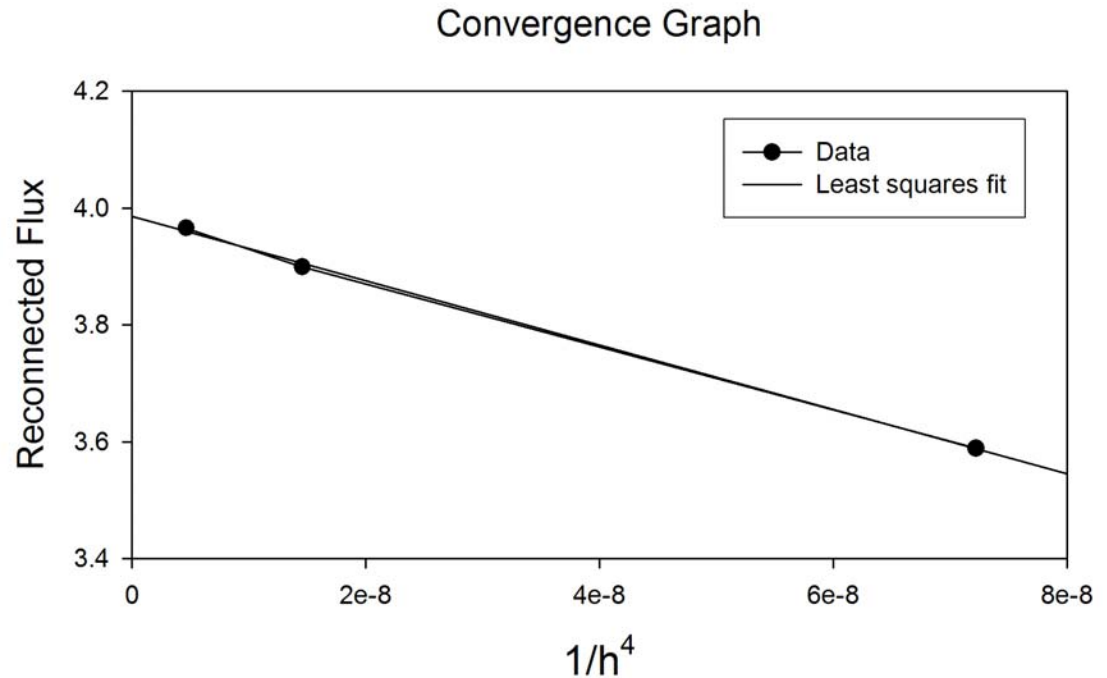
Now working on 180 x 180 and higher: Details for bassi.nersc.gov:

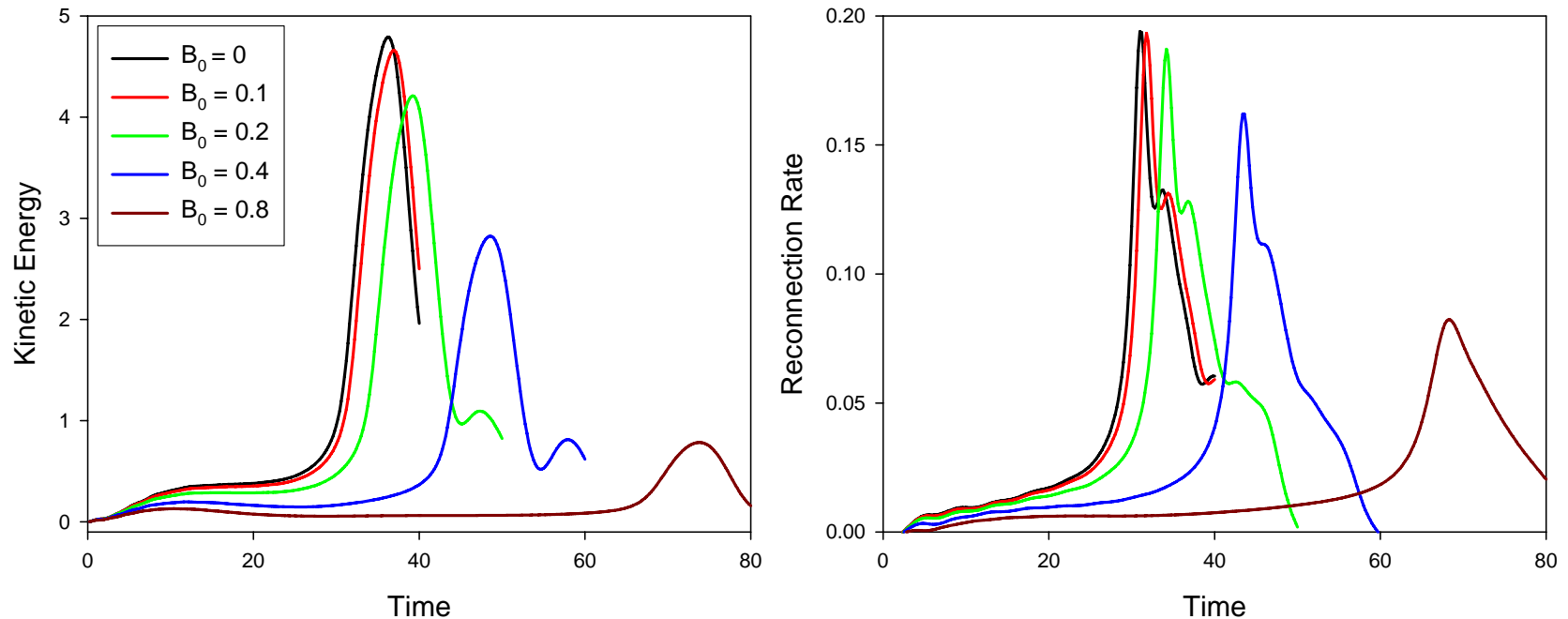| Mesh points	180 x 180
Matrix Rank	5.9×10^5
# Non-zeros	9.5×10^7
# NZ in L/U	8.8×10^8

# processors	8	32	128
Factor (s)	69.5	38.1	16.9
Gflop/s	27.2	50.1	112.8

Total problem time (8 processors) = 208 s x 400 cycles x 8p = 185 p-hrs

NOTE: mesh adaptation (almost implemented) should bring this down sharply
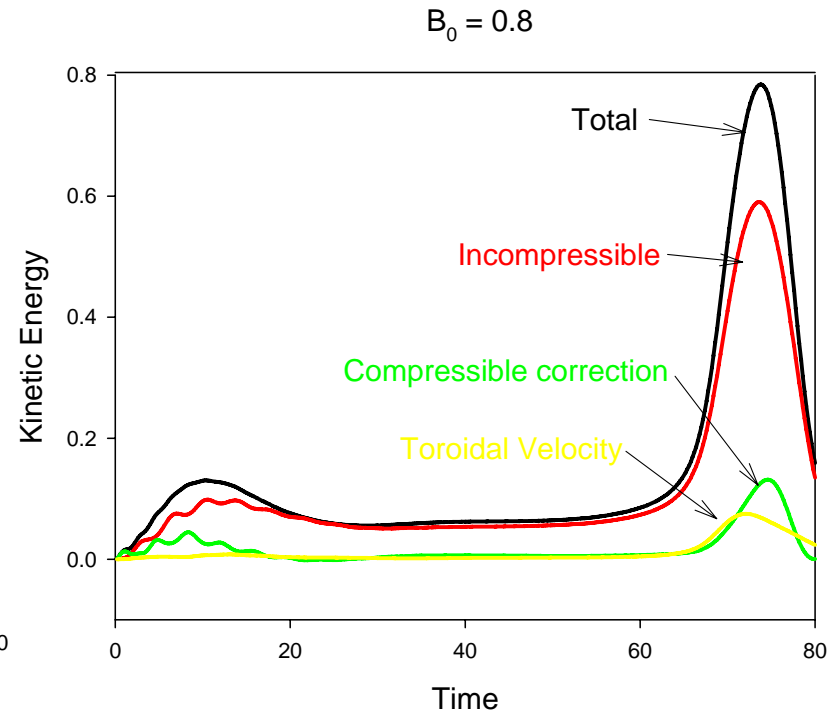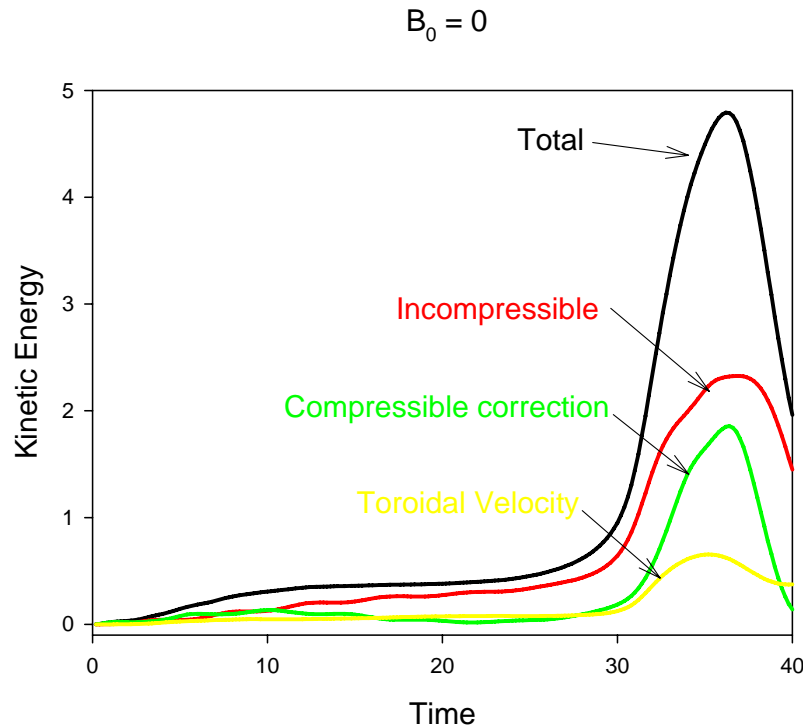
Effect of adding a guide field on 2-fluid reconnection

Effect of a Guide Field (into the paper)

- Adding a guide field delays transition time and reduces maximum reconnection rate

- Small effect for $B_0 < 0.2$

- To be studied further

Change in velocity field with toroidal field strength

- Velocity field becomes more like incompressible flow as toroidal field strength increases

Adaptive Meshing
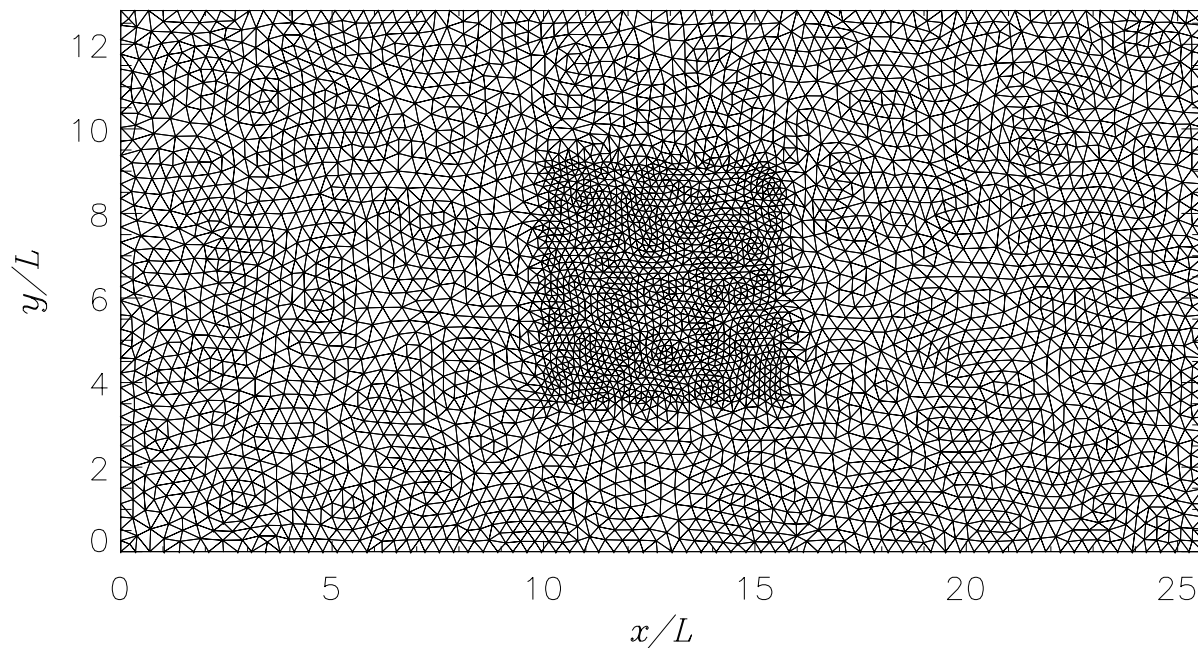
Andy Bauer (RPI) has implemented an arbitrary unstructured mesh in the M3D-C^1 code and is exploring different adaptive strategies. This greatly improves the efficiency of the 2-fluid reconnection problem.

Nonuniform mesh with resolution of 121x121 structured mesh near center gives same results as 121x121 calculation in 1/3 the time.
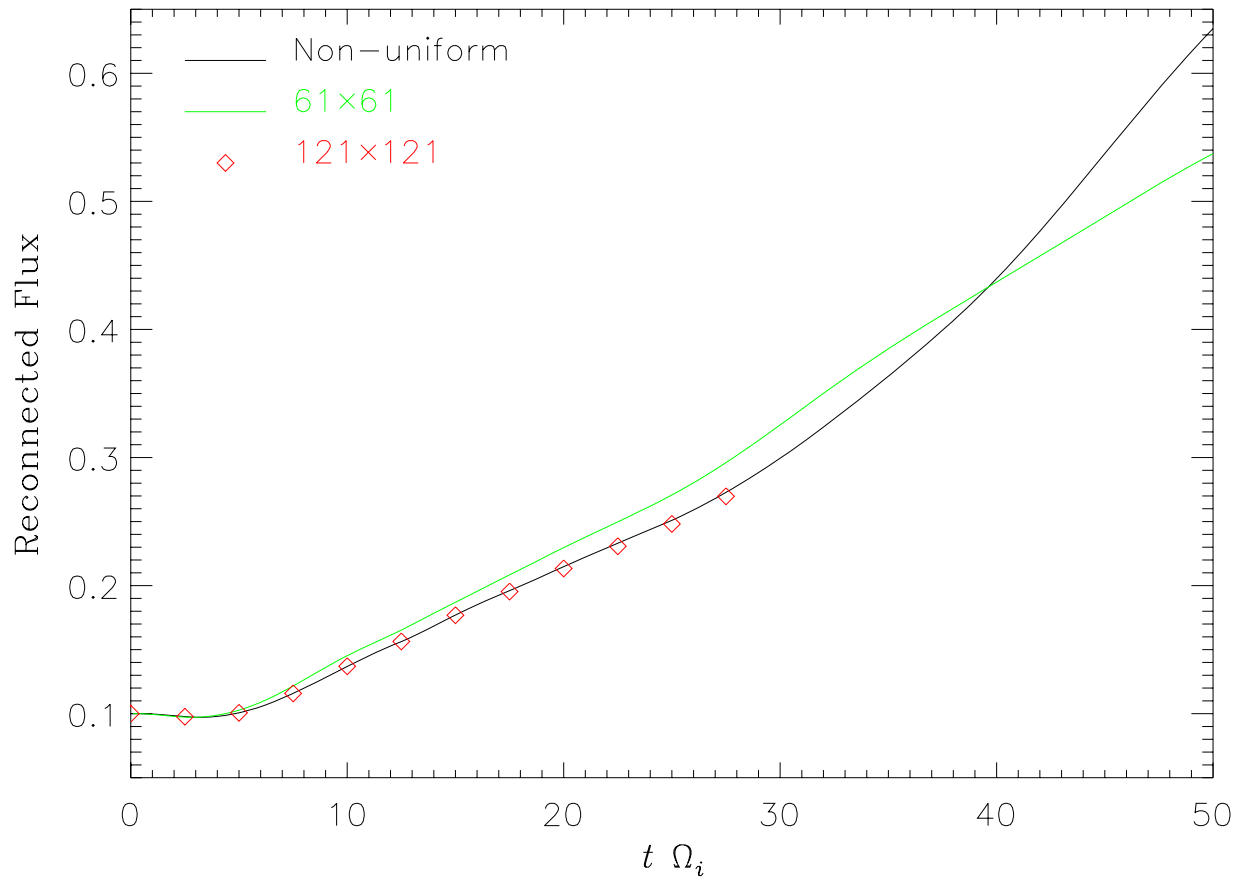
(4-field calculation)

Tests of the 2-fluid and Gyroviscous terms: Gravitational Instability

$$\times \quad \vec{B} = B_0 \hat{z}$$

$$\nabla \rho = \eta \rho \hat{y}$$

$$\sim e^{ikx}$$

$$\vec{g} = -g\hat{y}$$

Low-β result (R&T)

$$\omega^2 - \omega_* \omega + \gamma_{MHD}^2 = 0$$
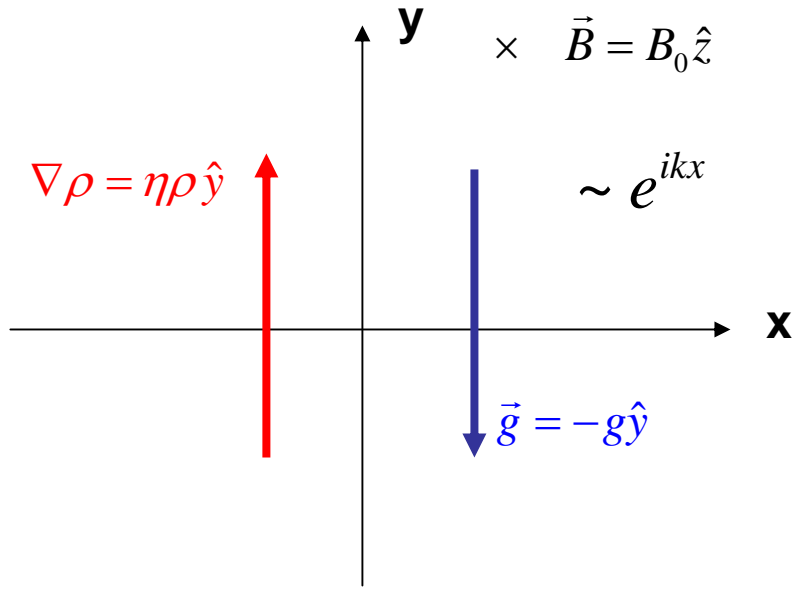
$$\omega_* = \omega_{*2F} + \omega_{*GV}, \quad \gamma_{MHD}^2 = \frac{g}{L}$$

$$\omega_{*2F} = \frac{gk}{\Omega}, \quad \omega_{*GV} = \frac{1}{2}\frac{\rho_i^2 k^2}{kL}\Omega$$

$$\frac{\partial \rho}{\partial t} + \nabla \bullet (\rho \vec{V}) = 0 \qquad\qquad p = p_i(\rho)$$

$$\frac{\partial \vec{B}}{\partial t} = \nabla \times \left[\vec{V} \times \vec{B} - \frac{1}{ne}\left(\vec{J} \times \vec{B} \right) \right] \qquad \vec{J} = \nabla \times \vec{B}$$

$$\omega = \frac{1}{2}\left(\omega_* \pm \sqrt{\omega_*^2 - 4\gamma_{MHD}^2} \right)$$

Stable if: $\omega_* > 2\gamma_{MHD}$

$$nM_i(\frac{\partial \vec{V}}{\partial t} + \vec{V} \bullet \nabla \vec{V}) + \nabla p = \vec{J} \times \vec{B} - \nabla \bullet \Pi_{GV}$$

Braginskii gyro-viscosity in M3D-C^1:

$$\nabla \cdot \ddot{\Pi} = \left\{ \left[\nabla \times \left(\frac{mp}{eB^2} \vec{B} \right) \right] \cdot \nabla \right\} \vec{V} - \nabla \left[\frac{mp}{2eB^2} \vec{B} \cdot \left(\nabla \times \vec{V} \right) \right] - \nabla \times \left\{ \frac{mp}{eB^2} \left[(B \cdot \nabla) \vec{V} + \frac{1}{2} \left(\nabla \cdot \vec{V} - \frac{3}{B^2} \vec{B} \cdot \left[(\vec{B} \cdot \nabla) \vec{V} \right] \right) \vec{B} \right] \right\}$$

$$+ (B \cdot \nabla) \left\{ \frac{mp}{eB^2} \left(\frac{3}{B^2} \vec{B} \times \left[(\vec{B} \cdot \nabla) \vec{V} \right] + \frac{3}{2B^2} \left[\vec{B} \cdot \left(\nabla \times \vec{V} \right) \right] \vec{B} - \nabla \times \vec{V} \right) \right\}$$

Ramos

$\hat{z} \cdot \quad \rightarrow \quad [V_z, \alpha I] - \alpha \left\{ [\psi, \nabla_\perp^2 U] + \left[\frac{\partial \psi}{\partial x}, \frac{\partial U}{\partial x} - \frac{\partial \chi}{\partial y} \right] + \left[\frac{\partial \psi}{\partial y}, \frac{\partial U}{\partial y} + \frac{\partial \chi}{\partial x} \right] \right\} - \frac{\partial \alpha}{\partial x} \left[\psi, \frac{\partial U}{\partial x} - \frac{\partial \chi}{\partial y} \right] - \frac{\partial \alpha}{\partial y} \left[\psi, \frac{\partial U}{\partial y} + \frac{\partial \chi}{\partial x} \right]$

$+ \frac{1}{2} \alpha \nabla_\perp^2 \chi \nabla_\perp^2 \psi + \frac{1}{2} \left(\alpha \nabla_\perp^2 \chi, \psi \right) - \frac{1}{2} \left[(\gamma \kappa, \psi) + \gamma \kappa \nabla_\perp^2 \psi \right] + [\gamma \xi_z, \psi] + \frac{1}{2} [\lambda I, \psi] + [\alpha \nabla_\perp^2 U, \psi]$

$-\hat{z} \cdot \nabla \times \quad \rightarrow \quad \left[\frac{\partial \chi}{\partial x} + \frac{\partial U}{\partial y}, \frac{\partial (\alpha I)}{\partial y} \right] - \left[\frac{\partial \chi}{\partial y} - \frac{\partial U}{\partial x}, \frac{\partial (\alpha I)}{\partial x} \right] + [\nabla_\perp^2 U, \alpha I] + \nabla_\perp^2 \left\{ \alpha [\psi, V_z] \right\} - \frac{1}{2} \nabla_\perp^2 \left(\alpha I \nabla_\perp^2 \chi \right) + \frac{1}{2} \nabla_\perp^2 \left(\gamma \kappa I \right)$

$+ \frac{\partial}{\partial y} [\gamma \xi_x, \psi] - \frac{\partial}{\partial x} [\gamma \xi_y, \psi] + \frac{1}{2} \left\{ \frac{\partial \lambda}{\partial x} \left[\frac{\partial \psi}{\partial x}, \psi \right] + \frac{\partial \lambda}{\partial y} \left[\frac{\partial \psi}{\partial y}, \psi \right] + ([\lambda, \psi], \psi) + [\lambda \nabla_\perp^2 \psi, \psi] \right\} + \frac{\partial}{\partial x} \left[\psi, \alpha \frac{\partial V_z}{\partial x} \right] + \frac{\partial}{\partial y} \left[\psi, \alpha \frac{\partial V_z}{\partial y} \right]$

$\nabla \cdot \quad \rightarrow \quad \left[\frac{\partial \chi}{\partial x} + \frac{\partial U}{\partial y}, \frac{\partial (\alpha I)}{\partial x} \right] + \left[\frac{\partial \chi}{\partial y} - \frac{\partial U}{\partial x}, \frac{\partial (\alpha I)}{\partial y} \right] + [\nabla_\perp^2 \chi, \alpha I] + \frac{1}{2} \nabla_\perp^2 \left\{ \alpha \left[I \nabla_\perp^2 U - (\psi, V_z) \right] \right\} + \frac{\partial}{\partial x} [\gamma \xi_x, \psi] + \frac{\partial}{\partial y} [\gamma \xi_y, \psi]$

$+ \frac{1}{2} [[\lambda, \psi], \psi] + \lambda \left[\frac{\partial \psi}{\partial y}, \frac{\partial \psi}{\partial x} \right] + \frac{1}{2} \frac{\partial \lambda}{\partial x} \left[\frac{\partial \psi}{\partial y}, \psi \right] - \frac{1}{2} \frac{\partial \lambda}{\partial y} \left[\frac{\partial \psi}{\partial x}, \psi \right] + \frac{\partial}{\partial x} \left\{ \alpha \left[\psi, \frac{\partial V_z}{\partial y} \right] \right\} - \frac{\partial}{\partial y} \left\{ \alpha \left[\psi, \frac{\partial V_z}{\partial x} \right] \right\} + [V_z, [\alpha, \psi]]$

$\alpha \equiv \frac{ep}{mB^2} = \frac{ep/m}{\left(\frac{\partial \psi}{\partial x} \right)^2 + \left(\frac{\partial \psi}{\partial y} \right)^2 + I^2}$

$\gamma = \frac{3ep/m}{\left[\left(\frac{\partial \psi}{\partial x} \right)^2 + \left(\frac{\partial \psi}{\partial y} \right)^2 + I^2 \right]^2}$

$\vec{\xi} = \left\{ \frac{\partial \psi}{\partial x} [\psi, V_z] + I \left[\psi, \frac{\partial \chi}{\partial y} - \frac{\partial U}{\partial x} \right] \right\} \hat{x}$

$+ \left\{ \frac{\partial \psi}{\partial y} [\psi, V_z] - I \left[\psi, \frac{\partial \chi}{\partial x} + \frac{\partial U}{\partial y} \right] \right\} \hat{y}$
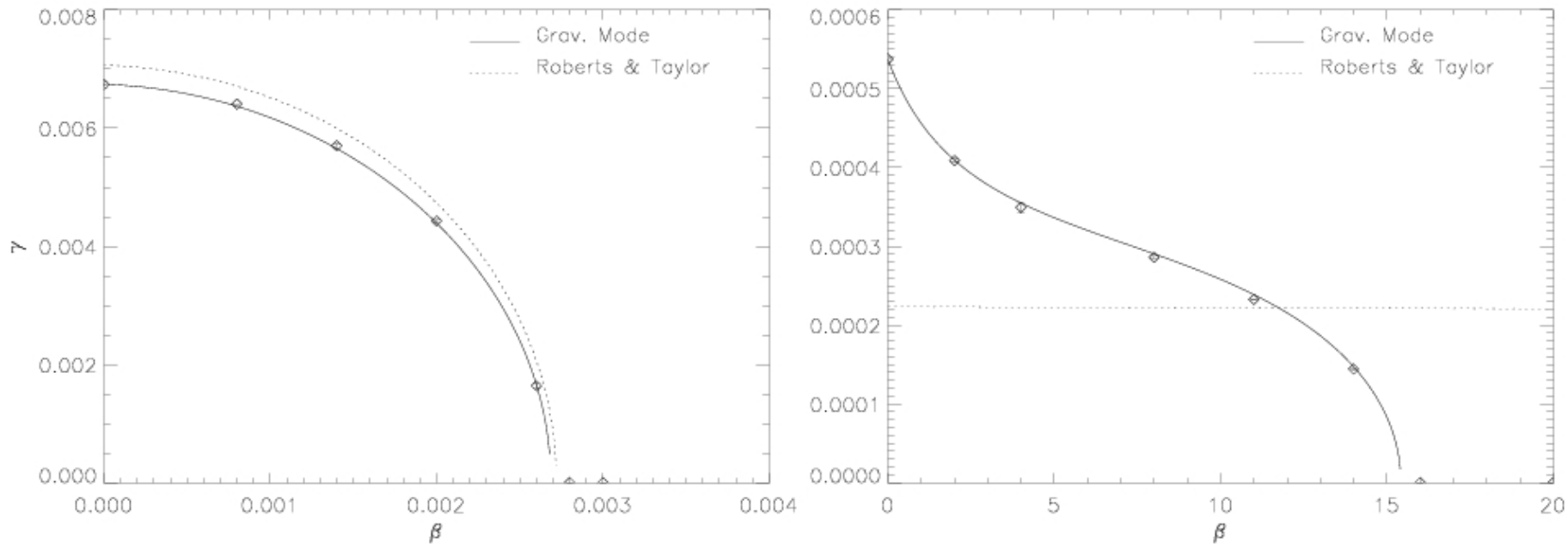
$\lambda = \gamma \left[(\psi, V_z) - I \nabla_\perp^2 U \right]$

$\kappa \equiv \frac{\partial \psi}{\partial y} \left[\frac{\partial \chi}{\partial x} + \frac{\partial U}{\partial y}, \psi \right] - \frac{\partial \psi}{\partial x} \left[\frac{\partial \chi}{\partial y} - \frac{\partial U}{\partial x}, \psi \right] + I [V_z, \psi]$

$- \left\{ \frac{\partial \psi}{\partial x} \left[\psi, \frac{\partial \chi}{\partial x} + \frac{\partial U}{\partial y} \right] + \frac{\partial \psi}{\partial y} \left[\psi, \frac{\partial \chi}{\partial y} - \frac{\partial U}{\partial x} \right] \right\} \hat{z}$
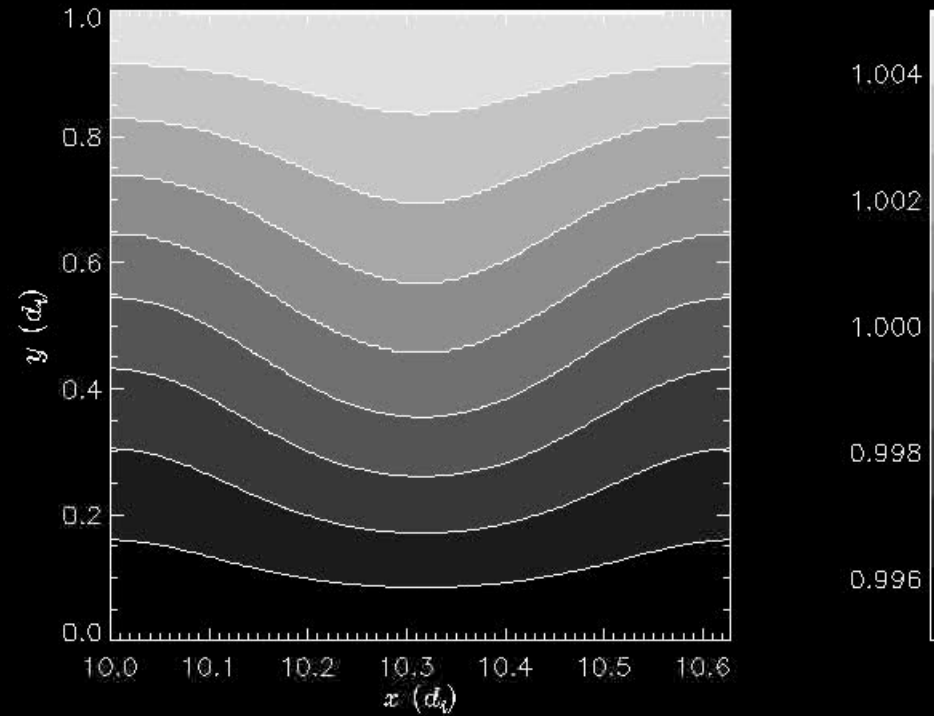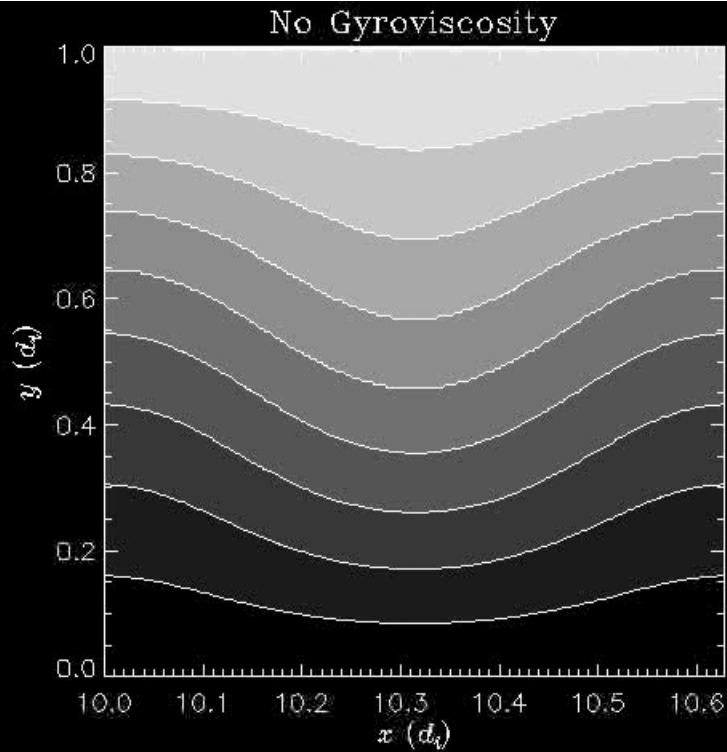
Breslau

M3D-C^1 Gravitational Instability stabilized by Gyroviscosity

We have calculated the stabilization of the gravitational
instability by Gyroviscosity: low beta (left) and high beta (right)

Ferraro

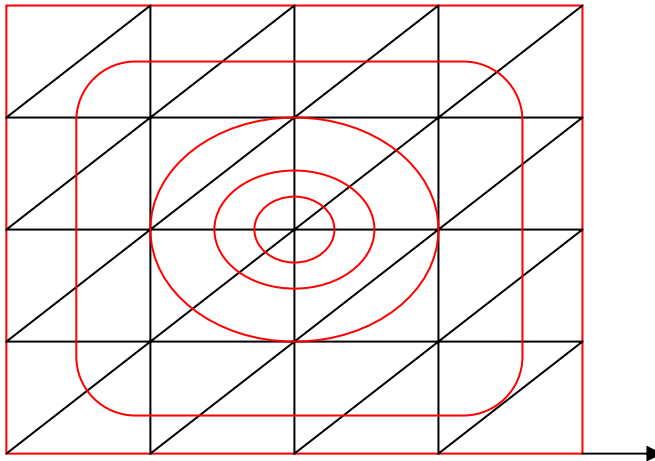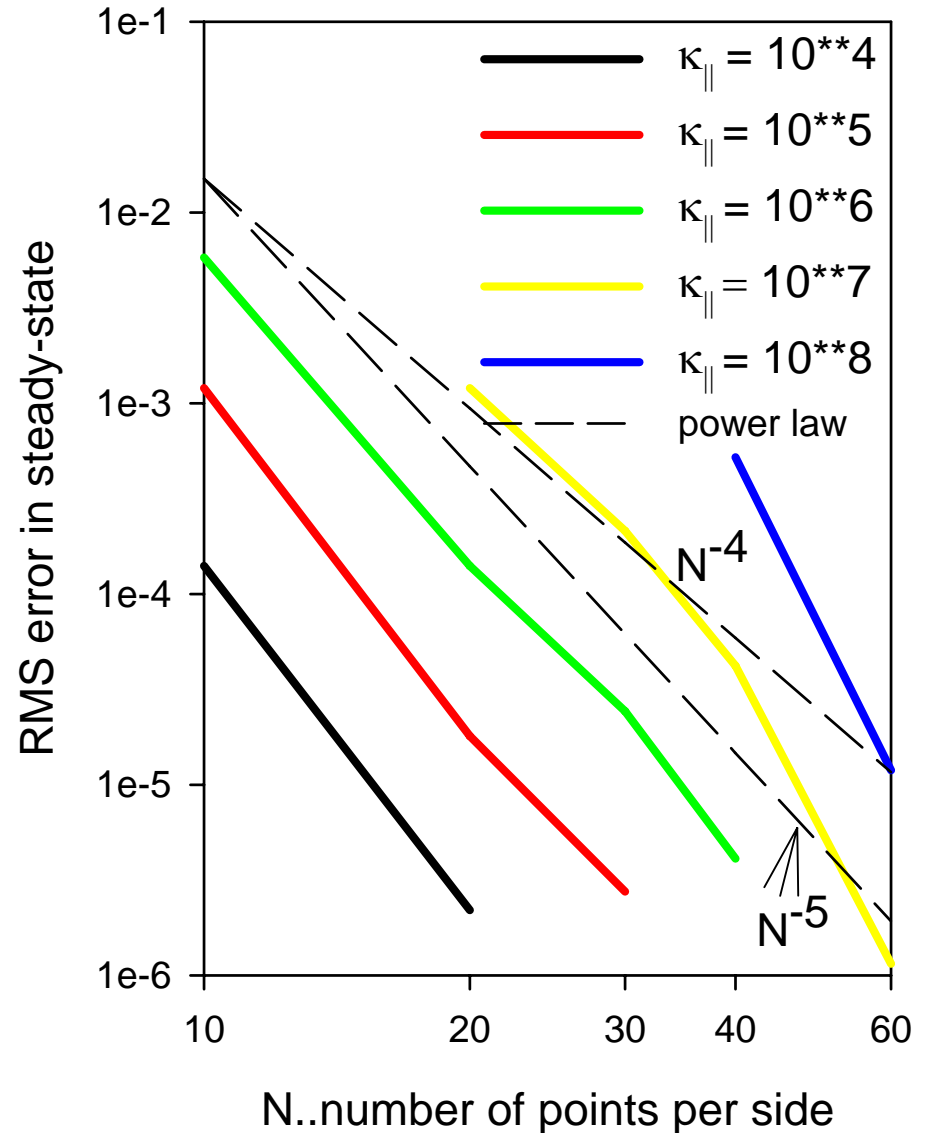# M3D-C^1...Gravitational Instability: nonlinear

Ferraro

Anisotropic Diffusion

Shows greater than N^{-5} convergence

$$\frac{\partial T}{\partial t} = \nabla \bullet \left[\kappa_\parallel \frac{\vec{B}\vec{B}}{B^2} \bullet \nabla T \right] + \nabla^2 T + S$$

Solve to steady state

$$S = \psi = \cos\frac{\pi x}{L}\cos\frac{\pi y}{L}$$

RMS error in steady-state vs N..number of points per side

- $\kappa_\parallel = 10^{**}4$
- $\kappa_\parallel = 10^{**}5$
- $\kappa_\parallel = 10^{**}6$
- $\kappa_\parallel = 10^{**}7$
- $\kappa_\parallel = 10^{**}8$
- power law

N^{-4}

N^{-5}

Summary and Conclusions

- Full 8-field E-MHD equations solved in 2D slab geometry with stream function/potential form

- Q_{18} elements allow high accuracy, compact representation of solution

- Implicit solution technique implies time step can be set by accuracy requirements, not stability

- 2-fluid reconnection problems require localized regions with high resolution…natural for adaptive refinement

- Now generalized to toroidal geometry (Ferraro)

- 3D extensions underway